

1 **Title**

2 Integrative analyses to investigate the link between microbial activity and metabolites
3 degradation during anaerobic digestion

4

5 **Author names + Affiliations**

6 Laetitia Cardona¹, Kim Anh Lê Cao², Francesc Puig-Castellvi^{1,3}, Chrystelle Bureau¹, Céline
7 Madigou¹, Laurent Mazéas¹, Olivier Chapleur^{1*}

8 ¹Université Paris-Saclay, INRAE, PROSE,

9 1 rue Pierre-Gilles de Gennes, CS 10030, 92761 Antony Cedex, France

10 ²Melbourne Integrative Genomics, School of Mathematics and Statistics, The University of
11 Melbourne, Parkville VIC 3010, Australia

12 ³Ingénierie, Procédés, Aliments research unit, AgroParisTech, INRA, Université Paris-Saclay,
13 1 rue des Olympiades, 91300 Massy, France

14

15 ***Corresponding author**

16 Tel + 33 1 40 96 65 06

17 olivier.chapleur@irstea.fr

18 <https://orcid.org/0000-0001-9460-921X>

19

20 **Abstract**

21 Anaerobic digestion (AD) is a promising biological process which converts waste into
22 sustainable energy. To fully exploit AD's capability, we need to deepen our knowledge of the
23 microbiota involved in this complex bioprocess. High-throughput methodologies open new
24 perspectives to investigate AD process at the molecular level, supported by recent data
25 integration methodologies to extract relevant information. In this study, we investigated the
26 link between microbial activity and substrate degradation in a lab-scale anaerobic co-digestion
27 experiment, where bioreactors were fed with 9 different mixtures of three co-substrates (fish

28 waste, sewage sludge, and grass). Samples were profiled using 16S rRNA sequencing and
29 untargeted metabolomics. In this article, we propose a suite of multivariate tools to
30 statistically integrate these data and identify coordinated patterns between groups of microbial
31 and metabolic profiles specific of each co-substrate. Five main groups of features were
32 successfully evidenced, including cadaverine degradation found to be associated with the
33 activity of microorganisms from the order *Clostridiales* and the genus *Methanosarcina*. This
34 study highlights the potential of data integration towards a comprehensive understanding of
35 AD microbiota.

36

37 **Keywords**

38 16S RNA sequencing; metabolomic; data integration; methanisation; co-digestion; Partial
39 Least Squares regression

40

41 **Introduction**

42 Deciphering the microbial communities in diverse domains, such as health, food safety
43 and environment, has been widely addressed by the development of high-throughput
44 technologies. In particular, Anaerobic Digestion (AD) bioprocess is constituted by extremely
45 complex microbial communities, mainly composed of bacteria and archaea, with high
46 functional redundancies. While AD is a promising bioprocess for the production of biogas, a
47 sustainable energy, from the degradation of organic waste, the key microorganisms driving
48 AD remain largely unknown. AD bioprocess involves four principal steps: hydrolysis,
49 acidogenesis, acetogenesis and methanogenesis. The optimal functioning of AD relies on the
50 efficient network between the microbes carrying successively these steps. However, the
51 microbial diversity and interactions between microorganisms are highly sensitive and depend
52 on multiple technical parameters such as temperature (Madigou et al., 2019; Noll et al., 2010),
53 presence of inhibitors (Li et al., 2017; Poirier et al., 2016; Sousa et al., 2013), or feedstock
54 composition (Zamanzadeh et al., 2017).

55 Emerging omics and high-throughput approaches can monitor microbial complexity
56 across multiple functional levels (Vanwonterghem et al., 2014). Metagenomics,
57 metatranscriptomics, metaproteomics and metabolomics provide necessary information
58 related to a community's genes, gene expression, proteins and metabolite production. They
59 reveal potential and activated functions of microbial communities. In our context, these omics
60 can unravel the intricate networks of functional processes of AD, especially when comparing
61 bioreactors under different operational conditions to elucidate their functioning (Carballa et
62 al., 2015; De Vrieze and Verstraete, 2016; Lü et al., 2014).

63 In parallel to the important advancements in these fields, the recent development of
64 specific statistical methods and user-friendly workflows has substantially improved the
65 analysis and visualisation of these omics results (Bouhlef et al., 2018; Callahan et al., 2016;
66 Rohart et al., 2017; Singh et al., 2019). As the statistical analysis of single omics is not
67 sufficient to decipher complex microbial relationships, the combination of information from
68 several data sources has become mandatory. Computational analytical methods have a rising
69 potential to capitalise on this rich data but they are still at their infancy and are not broadly
70 used for this type of problems. Classical multivariate methods, including Principal
71 Component Analysis (PCA) or Principal Coordinate Analysis (PCoA), have been widely used
72 for single omics datasets, such as 16S or metabolomic data (Poirier et al., 2016; Wang et al.,
73 2017). However, such methods are exploratory and do not fully characterised the microbial
74 communities playing a role in the biological systems being studied. Moreover, these methods
75 are not currently used to integrate information from different omics experiments. Novel
76 computational and statistical methods are becoming available to fully harvest the large
77 amount of data generated in multi-omics experiments (Lê Cao et al., 2009; Singh et al., 2019;
78 Straube et al., 2017). These methods aim to extract complementary information from several

79 datasets for a holistic understanding of the interplay between the different levels of
80 information.

81 Several AD studies have already shown the utility of using omics technologies to
82 decipher the anaerobic microbial population (Amha et al., 2018; Hassa et al., 2018). Analyses
83 of a single omics are routinely carried out (Bize et al., 2015; Cai et al., 2016) but the use of
84 several paired omics on the same samples, and their statistical integration are rare currently.
85 For example, Beale *et al.* applied metagenomic and metabolomic approaches to obtain new
86 insights on the diversity and activity of the anaerobic population after stress (Beale et al.,
87 2016) but no data integration was conducted between the two approaches. However,
88 correlation between transcriptomics and metabolomics has already been used to identify
89 important metabolites and genes for example in fungal or plants (Askenazi et al., 2003;
90 Hoefgen and Nikiforova, 2008).

91 Our study is the first of its kind in the anaerobic bioprocess field to investigate the link
92 between microbial activity from 16S rRNA sequencing data and patterns of substrate
93 degradation from metabolomics data. We propose a statistical framework to integrate these
94 datasets to identify associations, or correlations, between microbial activity and metabolites
95 specific of substrates degradation. To that end, 27 anaerobic bioreactors were fed with binary
96 mixtures of three substrates of different chemical composition (sludge and grass, or sludge
97 and fish) at different proportions. The microbial community was analysed through the
98 sequencing of the 16S rRNA-to characterise metabolically active microorganisms (De Vrieze
99 et al., 2018). The patterns of the substrate degradation were studied with untargeted
100 metabolomics using LC-MS, to determine the molecular fingerprints of waste degradation
101 (Villas-Bôas et al., 2006). Our statistical analyses revealed subsets of active microorganisms
102 highly associated to dynamics of substrate degradation over time, and enabled to posit novel
103 hypotheses regarding the capacity of microorganisms to degrade specific metabolites.

104

105 **Methods**

106 *Feedstock preparation*

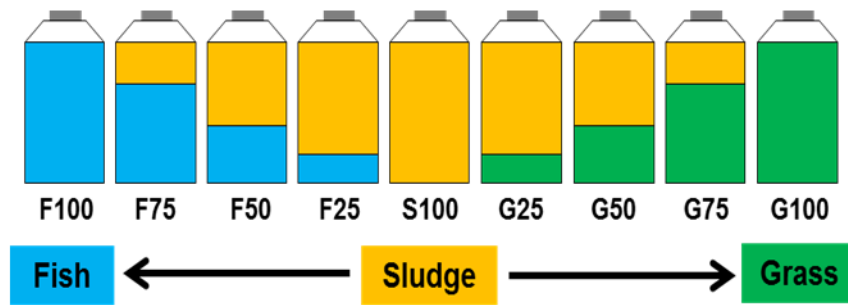
107 The inoculum used in the digestion experiments was sampled from a mesophilic full
108 scale industrial anaerobic bioreactor treating primary sludge from a wastewater treatment
109 plant (Valenton, France). The inoculum was incubated in anaerobic condition at 35°C without
110 feeding during 10 days in order to degrade the organic matter in excess before carrying out
111 the experiments.

112 Substrates used in the experiments were wastewater sludge collected from an industrial
113 wastewater treatment plant (Valenton, France), fish waste obtained from a fish shop, and
114 garden grass mowed from INRAE institute. Fish waste and garden grass were crushed and
115 kept at 4°C before carrying out the experiments.

116 *Bioreactors experimental set-up*

117 Binary mixtures of sludge with linearly decreasing percentages of either fish or grass
118 were prepared (0-100, 25-75, 50-50, 75-25, 100-0 respectively, see Figure 1). Experiments
119 were carried out in 1L glass bottles (700 mL working volume) at 35°C in the dark without
120 agitation. The same quantity of carbon was added in all the bioreactors, and the ratio of
121 substrate/inoculum used to feed and inoculate all the bioreactors was fixed at 12 gCOD/1.2
122 gCOD (Table S1). All bioreactors were complemented with a biochemical potential buffer
123 (International Standard ISO 11734 (1995)) to reach a final working volume of 700 mL. All
124 incubations were performed in triplicate. The bioreactors were then sealed with a screw cap
125 and a rubber septum and the headspaces were flushed with N₂ (purity >99.99%, Linde gas
126 SA). In total 27 anaerobic bioreactors were set-up.

127 In every reactor, 6 mL of liquid phase were sampled through the septum using a syringe
128 at a weekly frequency (days 0, 14, 21, 28). The collected samples were centrifuged at 10 000g
129 for 10 minutes to separate the supernatants from the pellets. Supernatants and pellets were
130 snap frozen using liquid nitrogen. Supernatants were kept at -20°C for metabolomics analysis
131 and pellets kept at -80°C for microbial analysis.



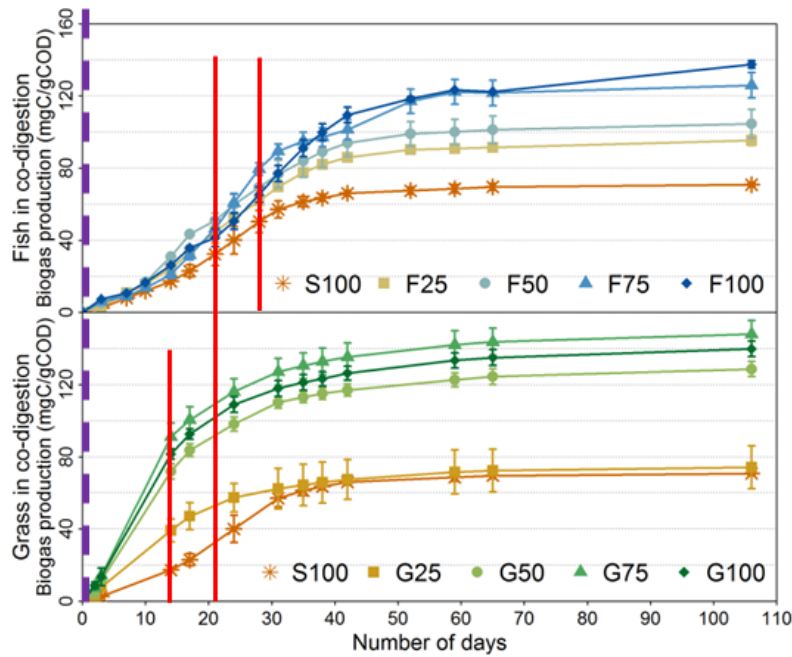
132

133 **Figure 1. Scheme of the batch experimental design.** S100 stands for bioreactors fed with
134 wastewater sludge alone, F25, F50, F75, F100 stands for bioreactors fed with 25, 50, 75 or
135 100% of fish (F) respectively, in co-digestion with sludge. G25, G50, G75, G100 stands for
136 bioreactors fed with 25, 50, 75 or 100% of Grass (G) respectively, in co-digestion with
137 sludge.

138

139 *RNA extraction and 16S rRNA sequencing*

140 Based on the biogas production, a total of 22 samples were selected (corresponding to
141 the highest biogas production as indicated in Figure 2). Since fish-fed bioreactors showed a
142 higher delay than grass-fed bioreactors before biogas production started, the sampling time-
143 points used were different for the two substrates (days 14 and 21 for grass-fed bioreactors,
144 and days 21 and 28 for fish-fed bioreactors, Figure 2).



145

146 **Figure 2. Cumulated biogas production (mgC/gCOD) over time (Days) for the different**
147 **bioreactors.** Mean values of the triplicate bioreactors are indicated with error bars
148 representing standard deviations within triplicates. Co-digestion percentage is described in
149 Figure 1, with either Fish (top) or Grass (bottom) co-digestion. Red solid lines indicate 16S
150 rRNA sequencing and metabolomics sampling dates. Purple dashed line corresponds to the
151 start of the incubation where an additional metabolomics analysis was carried out.

152

153

154 The commercial kit FastRNA Pro™ Soil-Direct (MP Biomedicals) was used to extract
155 the total RNA following the manufacturer's specifications. TURBO™ DNase (Ambion) kit
156 following the manufacturer's instructions allowed to remove DNA co-extracted. The RNA
157 was denatured by 2 min at 85°C in a dry bath and was then stored on ice. RNAClean XP
158 magnetic beads purification system (Beckman Coulter) was used to RNA purification by
159 adding 1.8 volumes of beads by volume of RNA. After mixing by pipetting and 5 min of
160 incubation, beads were captured using a magnetic rack on one side of the tube and then
161 washed by adding 500 µL of 70% cold ethanol (diluted in DEPC-water). Tubes were
162 incubated during 30 seconds at room temperature and ethanol was then removed. This
163 washing step was repeated 3 times. Once ethanol finally evaporated, beads were resuspended
164 with DEPC-water to eluted RNA from the beads. Finally, beads were removed using the
magnetic rack and RNA was recovered in the supernatant. The integrity and quantity of the

165 RNA was evaluated using High Sensitivity RNA ScreenTape and 2200 TapeStation (Agilent
166 Technologies) following the manufacturer's protocol.

167 A reverse transcription polymerase chain reaction (RT-PCR) was carried out on the
168 RNA using the mix iScript Reverse Transcription Supermix (Biorad) and the following
169 thermocycler program: 5 min at 25°C, 30 min at 42°C and 5 min at 85°C. The cDNA was
170 quantified using Qubit 2.0 fluorometer (ssDNA assay kit, Invitrogen, Life Technologies).

171 Archaeal and bacterial hyper variable region V4-V5 of the 16S rRNA gene were
172 amplified as cDNA, and these amplicons were then sequenced according to the protocol
173 described by Madigou *et al.* (Madigou et al., 2019). The raw sequences were deposited in the
174 NCBI databases under the project accession number PRJNA562430.

175 FROGS (Find Rapidly OTU with Galaxy Solution), a galaxy/CLI workflow (Escudié et
176 al., 2018), was used to generate an OTU count matrix. R CRAN software (version 3.5.1) was
177 used for alpha diversity analysis with Shannon method using phyloseq R package (version
178 1.20.0). Proportions of archaeal and bacterial OTUs abundances were scaled per sample and
179 OTUs that exceeded 1% in terms of relative abundance in at least one sample, were selected
180 for the remainder of the analysis and square-root transformed.

181 *Metabolomics analysis*

182 Metabolomics analysis was performed on all collected supernatants. Samples were
183 analysed using reverse phase liquid chromatography coupled to high resolution mass
184 spectrometry (HPLC-ESI-HRMS) using a LTQ-Orbitrap XL instrument (Thermo Scientific).
185 Samples were diluted at 1/10 in MilliQ water and 10 µL of the solution was injected into the
186 analytical system. Chromatographic separation was performed on Accela 1250 pump at 400
187 µL/min with a linear gradient from 10 to 80% of mobile phase A (acetonitrile + 0.05% formic
188 acid) and 90 to 20 % of mobile phase B (water + 0.05% formic acid) into a SynchronisTM C18
189 column (50x2.1 mm, 1.7µm, Thermo Scientific) during 23 minutes, followed by a

190 stabilisation phase of 5 minutes to return at the initial condition. After chromatographic
191 separation, the sample was ionized by electrospray ionization (ESI) on positive mode. The
192 detection was performed in full scan over an m/z range from 50 to 500 at a resolution of 100
193 000. A sample consisting of the supernatant from the digestion of anaerobic sludge was used
194 as a quality control and injected every 10 experiment samples. Blank samples were injected
195 every 10 samples, and an equimolar mix of the samples was injected every 5 samples.

196 The raw data obtained from the LC-HRMS analyses were transformed into mzXML
197 files using MSConvert (ProteoWizard 3.0). The XCMS R package (version 1.52.0) was used
198 to process the data (Smith et al., 2006). The method *centWave* was used to determine
199 chromatographic peaks (region of interest - ROIs) with a m/z error of 10 ppm and a peakwidth
200 between 20 and 50 seconds. The ROIs found in different samples were grouped using the
201 group method with a bandwidth of 30. Retention times from the same ROI groups were
202 unified across samples using the *orbiwarp* method. A second grouping was carried out using a
203 bandwidth of 25. Finally, missing ROIs in the samples were filled using the *fillPeaks* method.
204 Initial metabolite identification was performed based on the comparison of the accurate
205 molecular mass measured by LC-HRMS with the corresponding values found in the online
206 databases HMDB, LipidMaps, and PubChem (Fahy et al., 2007; Lee et al., 2018; Wishart et
207 al., 2018). In addition, for selected compounds, a confirmation of the metabolite identification
208 was performed by MS/MS fragmentation, and followed by the comparison of the acquired
209 MS/MS spectra with the theoretical spectra from the online databases HMDB and MassBank
210 (Horai et al., 2010).

211 *Statistical analysis and data integration*

212 Multivariate data analysis was carried out using the mixOmics R package' using a suite
213 of component-based methods to identify groups of microorganisms and metabolites
214 degradation with coordinated patterns.

215 First, each dataset was analysed independently using an exploratory (unsupervised)
216 approach, or a supervised approach to identify key OTUs and metabolites prior to data
217 integration as follows.

218 *Unsupervised analysis on the 16S data.* Sparse Principal Component Analysis (sPCA, (Shen
219 and Huang, 2008)) was applied on all the samples of the microbial dataset (16S rRNA, 22
220 samples) to evidence main sources of variation and identify OTUs that most contribute to
221 each principal component. Briefly, sPCA is based on PCA that includes a LASSO penalty for
222 variable selection. In our context, the main source of variation correspond to specific feeding
223 conditions (see Figure 3), and thus variable selection from sPCA enables us to identify
224 microorganisms characteristic of co-substrate.

225 *Supervised analysis on the metabolomic day 0 data.* Sparse Partial Least Squares
226 Discriminant Analysis (sPLS-DA, (Lê Cao et al., 2011)), a supervised classification method,
227 was applied on the mono-digestion samples (S100, F100, G100, 9 samples in total) at day 0 in
228 order to determine the molecules specific to each substrate before any degradation. PLS-DA
229 classifies samples into groups (sludge, fish, grass) and the sparse variant identifies metabolites
230 discriminating each co-substrate at the start of the experiment. This method has already been
231 used in metabolomics data analysis and successful in removing noise by selecting the most
232 informative variables (e.g. Jiang et al., 2014).-Classification performance was assessed based
233 on the mean classification error rate using leave-one-out cross-validation, and Mahalanobis
234 distance for prediction of the class of the samples (Rohart et al., 2017).

235 *Clustering.* Once selected, the abundances of the OTUs and the metabolites selected with
236 sPCA and sPLS-DA respectively were clustered using hierarchical clustering (using Ward's
237 method and Manhattan and Euclidean distances respectively for each data type), then
238 represented in heatmaps (heatmap.2 function from gplots R package, version 3.0.1).

239 *Data integration of the selected OTUs and metabolites.* The aim of this analysis is to identify
240 patterns of different variables (microbes and metabolites) characteristics of the different
241 conditions. Thus, this analysis included all 22 samples representative of the different feeding
242 conditions. We calculated the metabolite degradation rate data as the ratio between the
243 metabolites abundances at days 14, 21 or 28, relative to day 0. Both datasets were then
244 integrated using Partial Least Square (PLS) regression method with a canonical mode (Lê Cao
245 et al., 2009) to identify groups of OTUs and degraded metabolites that are highly correlated.
246 Briefly, PLS weights variables from both datasets optimally using loading vectors, so that
247 their linear combination (called PLS components) is maximally correlated and thus extract
248 similar patterns across datasets (see supplemental figure S2 A and B). Loading vectors
249 correspond to the weight assigned to each variable to define the PLS components. We
250 subsequently applied hierarchical clustering on the loadings vectors to identify clusters of
251 metabolites and OTUs variables with similar patterns of degradation rate or activity across the
252 different types of substrate mixtures. As the correlation structure between high-throughput
253 datasets can be highly spurious, we then further assessed the strength of the association
254 between the variables assigned to each cluster using the proportionality distance (R package
255 *propr* (Quinn et al., 2017)). We compared the distance between the profiles of each variable
256 within one cluster and to the distance between the profiles outside this cluster. A small
257 distance between two variables indicates a strong association.

258

259 **Results and discussion**

260 *Influence of the feeding composition on the biogas production*

261 We examined the cumulated biogas production in the different mixtures. Three main
262 results can be observed from Figure 2. Firstly, the sludge mono-digestion produced a lower
263 biogas quantity compared to the fish and grass mono-digestion. Secondly, the grass mono-

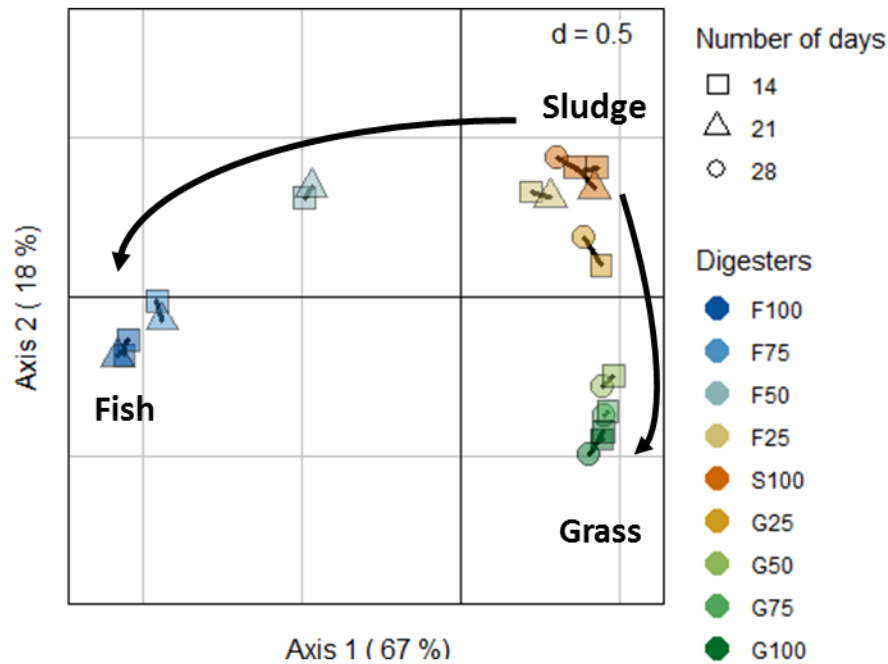
264 digestion provided the best biogas production performances, as the biogas production rate and
265 the final biogas production were higher than in fish mono-digestion. Thirdly, compared to
266 sludge mono-digestion, the biogas production in bioreactors with mixtures of waste presented
267 two patterns of improvement according to the type of co-substrate (fish or grass). In co-
268 digestion with fish, the biogas production from the sludge improved linearly with the increase
269 of fish quantity in the feedstock composition. In co-digestion with grass, the final biogas
270 production was improved only when at least 50% of grass was present in the feedstock
271 composition. A comparison of the major chemical parameters of anaerobic digestion has been
272 already described in a precedent study (Cardona et al., 2019). In the present study, we focus
273 on the influence of the feedstock composition on microbial activity and its relation with
274 degradation of specific metabolites.

275 *Influence of the feeding composition on the microbial community*

276 The influence of the feeding composition on the microbial diversity was evaluated using
277 the Shannon index calculated on archaeal and bacterial communities (supplemental Figure
278 S1). The bacterial diversity was inversely proportional to the amount of fish present in the
279 bioreactors, while the level of the bacterial diversity remained stable when grass was present
280 in co-digestion with sludge. The archaeal diversity decreased sharply with the presence of fish
281 in the feedstock, or with high amount of grass. The low microbial diversity induced by the
282 presence of fish can be explained by the composition of a simpler substrate (in terms of
283 molecular variety) compared to the other substrates, or by a lower functional redundancy of
284 the microorganisms that can degrade fish substrate compared to those that can degrade grass
285 or sewage sludge.

286 Sparse PCA highlighted the main sources of variability in the 16S rRNA data set, while
287 identifying key OTUs driving this variation. We selected 43 OTUs, which in combination
288 explained 67 (first component) to 85% (two components) of the total microbial community

289 variance in the data. The sample plot in Figure 3 showed the strong influence of the feeding
290 composition on the microbial community. The samples were regrouped according to the
291 major co-substrate, and regardless of the sample collection time. This result suggests that the
292 variance due to time within conditions is low, and active microbial community over time is
293 relatively stable.



294
295 **Figure 3.** Microbial dynamics over time with respect to the different feeding
296 compositions. Sample plot from the sPCA from the 16S rRNA dataset. Bioreactors are
297 represented by colours and number of days by symbols.

298
299 The relative abundance of the selected microorganisms was compared between the
300 different mixtures (Figure 4). We observed differences in the active archaeal community
301 depending on the feeding type. Fish mono-digestion (F100) was mostly driven by the archaea
302 *Methanosarcina* OTU_6 and *Methanoculleus* OTU_18; grass mono-digestion (G100) by
303 *Methanospirillum* OTU_24, *Methanosarcina* OTU_1, *Methanofollis* OTU_64 and sludge
304 mono-digestion (S100) by *Methanosarcina* OTU_1, *Methanobacterium* OTU_63 and 204 and
305 two OTUs of *Methanoculleus* (18 and 50). With the exception of *Methanosarcina* which can

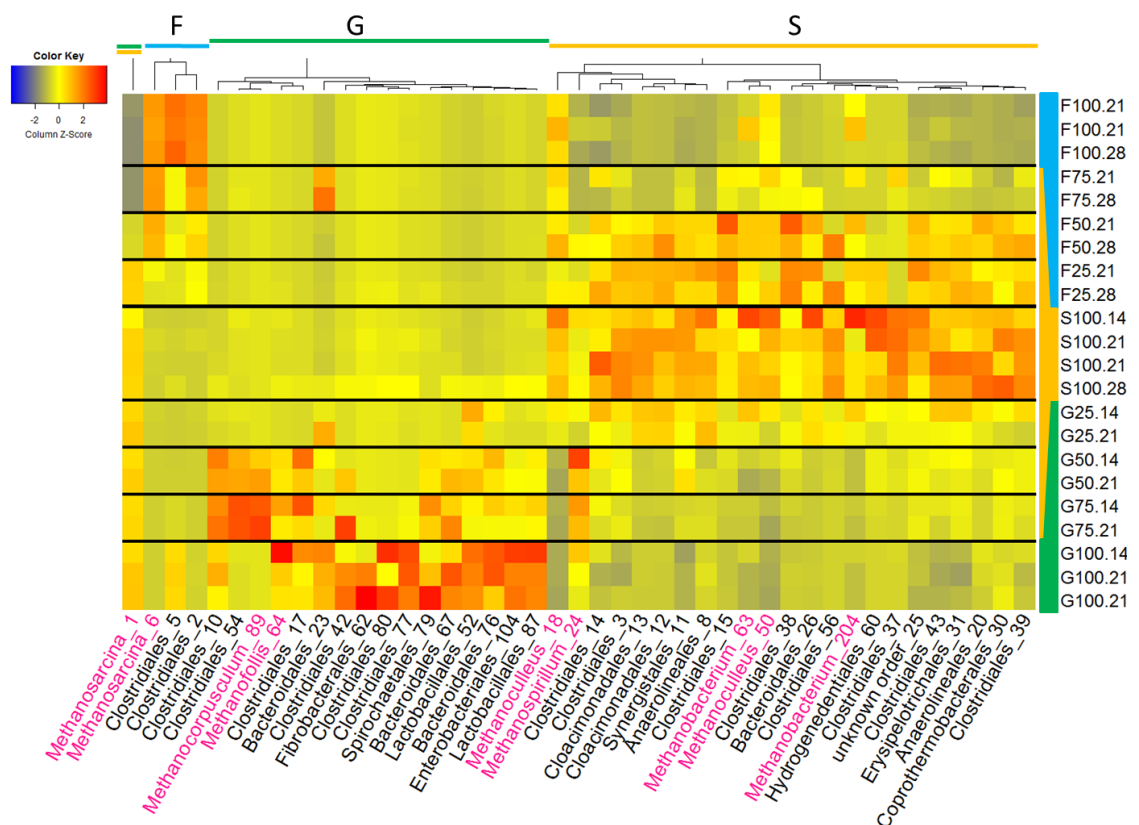
306 use different methanogenesis pathways, all the identified archaea only use the
307 hydrogenotrophic pathway to produce methane. The archaea composition is likely to depend
308 on the environmental conditions in the bioreactors induced by the different feeding conditions
309 and from bacterial dynamics. The fish substrate induced the activity of a specific OTU of
310 *Methanosarcina* that was not found in the other substrates. As *Methanosarcina* presents a
311 versatile methanogenesis metabolism, the modification of the OTU between the substrate
312 could reflect the use of different methanogenesis metabolism.

313 The diversity in the bacteria community also differed between feeding types. As
314 observed in the alpha diversity analysis, the fish substrate induced a lower microbial diversity
315 than grass or sludge. In fish mono-digestion, the order *Clostridiales*, grouping cellulolytic
316 degraders and fermentative members, represented more than 90% of the bacterial community
317 while the abundance reached 25% and 50% for respectively sludge and grass mono-digestion.
318 In grass mono-digestion, the abundance of *Spirochaetales*, *Fibrobacterales*, *Lactobacillales*
319 and *Enterobacteriales* was higher than in fish and sludge mono-digestion. They were
320 probably favoured by their ability to degrade cellulolytic substrates such as grass. Bacterial
321 community of sludge mono-digestion was mostly composed by *Cloacimonadales*,
322 *Synergistales*, *Anaerolineales*, *Hydrogenedentiales*, *Erysipelotrichales* and
323 *Coprothermobacteriales*. Members from the orders *Synergistales*, *Cloacimonadales*,
324 *Coprothermobacteriaceae* and *Anaerolineales* are known or suspected to be able to form
325 syntrophic interaction with hydrogenotrophic methanogens (Calusinska et al., 2018; Gagliano
326 et al., 2015; Ito et al., 2011; Sekiguchi et al., 2001). *Hydrogenedentiales* are H₂-utilising
327 bacteria and associations with the H₂-producers *Coprothermobacteriaceae* were evidenced
328 (Nobu et al., 2015). In sludge, the abundance of potential syntrophic partners in presence with
329 hydrogenotrophic methanogens suggests that methane production was mainly produced from

330 the hydrogenotrophic methanogenesis pathway, in line with the archaeal community
 331 described in this incubation.

332 In light of the current literature, the type of substrate used to feed the bioreactors has
 333 been suggested to contribute to the development of an adapted microbial community of
 334 degraders (De Francisci et al., 2015; Lee et al., 2018). Specifically, in our study, fish substrate
 335 was found to induce not only a low microbial diversity, but also the growth of a specific
 336 community compared to what was observed in grass and in sludge substrates. Indeed, only
 337 5% of the selected OTUs were common between fish- and sludge-bioreactors, 9% between
 338 both fish- and grass-bioreactors, while 17% of the selected OTUs were common between both
 339 grass- and sludge-bioreactors.

340



341

342 **Figure 4.** Heatmap of the microorganisms whose abundance contributes most to
 343 variance due to feeding composition selected with sPCA. The type of substrate used, day,
 344 duplicates were carried out on the bioreactors containing only fish, grass or sludge at day 21.

345 Taxonomy completed by the OTU number is indicated at the genus level for archaea (pink)
346 and at the order level for bacteria (black). Abundance is represented in the heatmap ranging
347 from blue (low) to high (red).
348

349 Within the mixtures, the abundance of the selected microorganisms changed with
350 feeding composition. However, microbial activity did not necessarily increase with the
351 amount of mixture proportions. For example, the relative abundances of the OTUs identified
352 as active in the fish:sludge mixture at 75:25 (F75) were similar to the relative abundances of
353 the same active OTUs in the fish mono-digestion (F100). As the proportion of sludge
354 increased, the active microorganisms more characteristic of sludge increased as well.
355 However, in grass mixtures, the active microbial community from sludge remained dominant
356 regardless the proportion of grass used (e.g down to 25% in the mixture with 75% of sludge,
357 G25). However, some microorganisms were found in specific proportions of grass:sludge. For
358 example, *Methanocorpusculum* and specific OTUs of *Clostridiales* were found in the mixes
359 50:50 and 75:25 of grass:sludge.

360

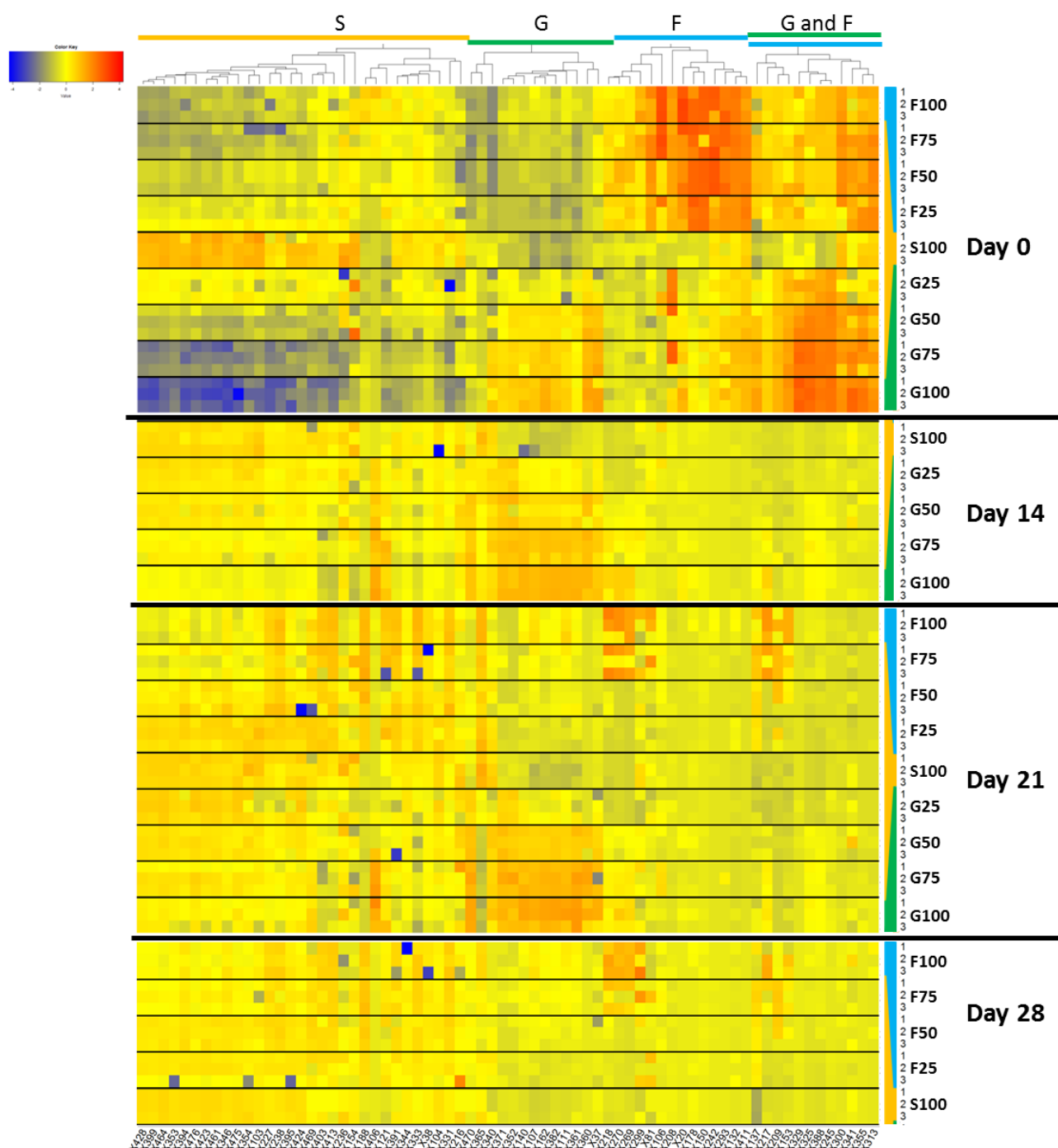
361 *Substrates degradation dynamics*

362 We studied the temporal dynamics of degradation of the different substrate mixtures by
363 analysing the metabolic fingerprint of the degradation in the bioreactors using an HPLC-ESI-
364 HRMS instrument. After data examination with XCMS, a total of 267 regions of interest
365 (ROI) were detected. ROI designate chromatographic features (m/z) in the spectrum. Sparse
366 PLS-DA identified 70 ROIs out of the 267 ROIs specific to each substrate (sludge, grass, fish)
367 initially present at day 0. The classification error rate from the sPLS-DA was 0, indicating that
368 all samples could be perfectly assigned to their respective groups using leave-one-out cross
369 validation based on these 70 ROIs. The ROIs were then clustered into four groups according
370 to their intensities at day 0. The degradation pattern of the selected ROIs was then examined
371 for every mixture across all time points. Four main degradation patterns were observed

372 (Figure 5). Three of these groups include the ROIs whose relative intensities were high only
373 in sludge-, grass- or fish-fed bioreactors (indicated as S, G, and F, respectively, in Figure 5) at
374 day 0. The other group (G and F) include the ROIs whose relative intensities were high in
375 both fish- and grass- but low in sludge-containing bioreactors at day 0.

376 Whilst the ROIs were selected to discriminate only mono-digestion at day 0, we
377 observed that the intensity of the ROIs differed across all feeding types. This result was
378 expected given the differences in the molecular composition of the substrates. In general, the
379 intensity of the ROIs representative of sludge decreased when fish or grass was mixed with
380 sludge. We also observed some temporal dynamics, as that the intensity of some ROIs
381 decreased over time, while some other either increased or remained stable during the
382 experiment. This can be explained as some metabolites may not be easily degraded, or may be
383 a product of degradation of other metabolites.

384



385

386 **Figure 5. Metabolites dynamics within bioreactors and over time.** The most discriminant
387 ROIs for the different co-substrates were selected by sPLS-DA at day 0, then clustered with
388 hierarchical clustering according to day 0. The profiles for the remaining days were then
389 represented in the heatmap based on the intensities. The different panels represent days 21-28
390 for bioreactors containing fish, 14-21 for bioreactors containing grass and 14-21-28 for
391 bioreactors containing sludge. For each waste mixture and date, triplicates bioreactors
392 numbered 1, 2 and 3 are indicated. Intensity ranges from blue (low) to red (high).
393

394 The putative identification of the ROIs based on their m/z is given in the Table S2. Out
395 of the 70 selected ROIs, 19 metabolites were identified, whilst the rest could not be assigned.
396 The metabolites assignment step in MS metabolomics analysis is a traditional bottleneck
397 (Longnecker et al., 2015). Our study was further hampered by the high structural diversity of
398 the compounds found in bioreactors, the lack of databases specific for anaerobic digesters,
399 and the absence of relevant literature of metabolomics analysis on anaerobic bioreactors.
400 However, the metabolites identified in the different clusters were biologically consistent with
401 the corresponding substrates. For example, metabolites identified in sludge-containing
402 samples were diethylthiophosphate (X340) and 6-methylquinoline (X218 and X270).
403 Diethylthiophosphate is a common degradation product of organophosphorus pesticides,
404 while 6-methylquinoline is a flavouring ingredient found in tea. Metabolites characteristics of
405 grass-fed bioreactors were plant constituents (betaine, X245), metabolites obtained from
406 lignin degradation (trans-ferulic acid and p-coumaric acid, X388 and X365, respectively), and
407 metabolites from sugar metabolism (galactitol, X329). In fish-fed bioreactors, most of the
408 metabolites corresponded to organic compounds resulting from amino acids degradation
409 (cadaverine and histamine, X132 and X150, respectively).

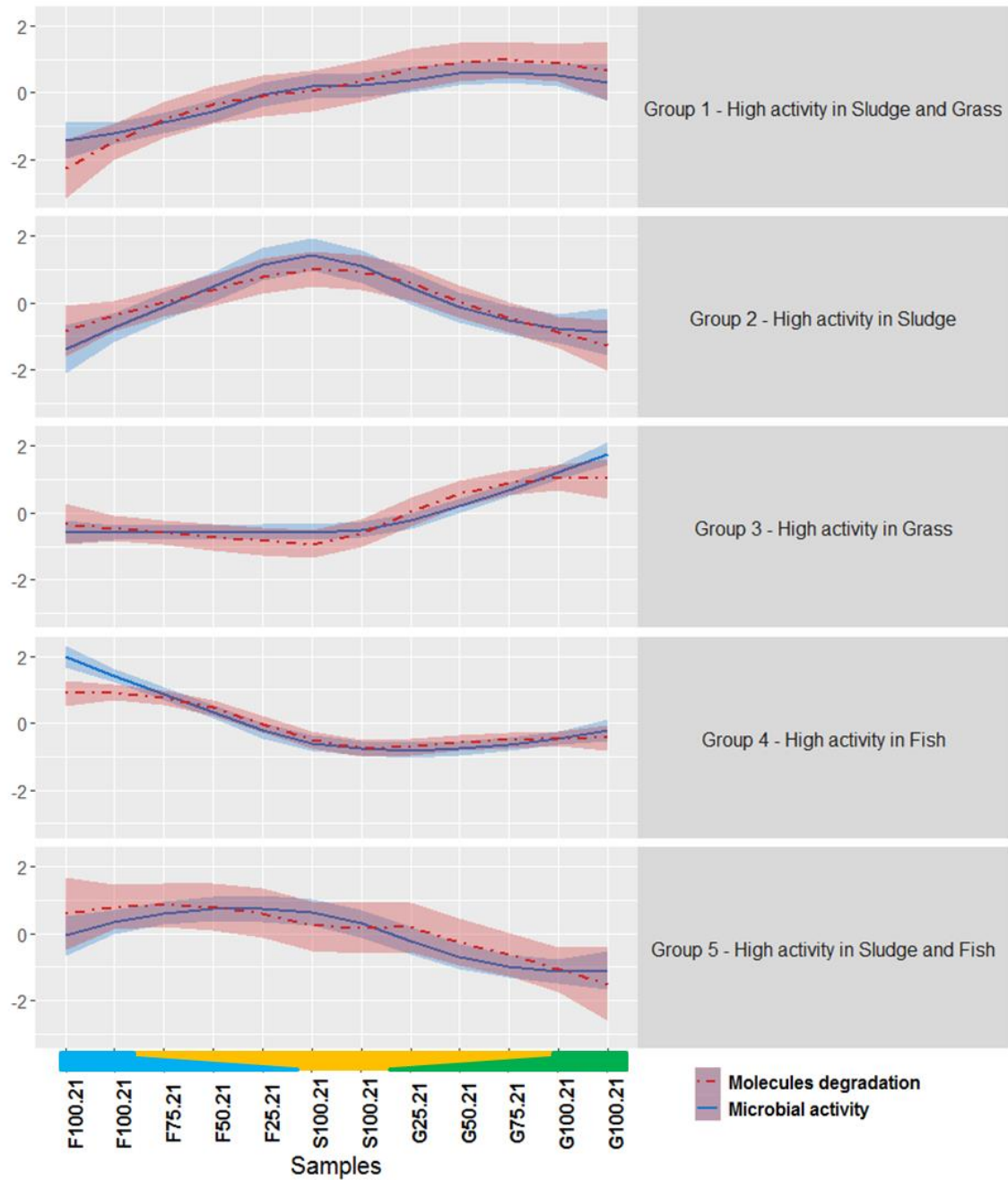
410

411 *Correlation between microbial activity and substrates degradation pattern*

412 Statistical data integration analysis was carried out between the microbial and
413 metabolites datasets to identify potential degraders of specific metabolites. As far as we know,
414 this type of analysis has never been applied in the anaerobic digestion field. Correlation
415 studies have been used to relate metabolite profiles to microbiome in gut studies (Han et al.,
416 2019; McHardy et al., 2013). For example, Han et al (2019) estimated the correlation between
417 cecal compounds and bacteria profiles acquired respectively by LC/MS and 16S RNA
418 sequencing analyses using Spearman's correlation. However, in datasets containing a large

419 number of variables, such approach is highly likely to result in spurious correlations. One
420 novelty in our study is to use component-based approaches, such as multivariate PLS method
421 that are well suited for a high correlation structure within and between datasets, whilst being
422 able to highlight key associations between variables from each dataset.

423 As described in the methods section, we considered the metabolites degradation rates
424 relative to day 0 in our analysis. The sample (ordination) plots from PLS (Figure S2 A-C)
425 show similar patterns for microbial and metabolites datasets, suggesting that an underlying
426 correlation structure between the two datasets exists and can be extract with such method. The
427 correlation circle plot (Figure S2 D) projects the variables into the space spanned by the PLS
428 components to visualise simultaneously the active microorganisms and the metabolites
429 responsible for this ordination of the samples (González et al., 2012). In particular, active
430 microorganisms and metabolites with a high degradation rate projected close to each other on
431 this graph are correlated, as they contribute equally to define the PLS components. A
432 hierarchical clustering was performed on the PLS loadings of the microbial and metabolites
433 variables. It helped to further identify groups of microorganisms potentially associated with
434 the metabolites degradation. In total, five clusters were evidenced.



435

436 **Figure 6.** Correlated dynamics of the active microorganisms and metabolites
437 **degradation across all samples at day 21.** Lines represent the mean values of the different
438 microbial activity (solid blue line) or metabolites degradation rates (dashed red line) for each
439 of the clusters identified using hierarchical clustering performed on the PLS loadings.
440 Shadows represent standard deviation. S100 stands for wastewater sludge alone, F25, F50,
441 F75, F100 stands for respectively 25, 50, 75 or 100% of fish (F) in co-digestion with sludge,
442 G25, G50, G75, G100 stands for respectively 25, 50, 75 or 100% of Grass (G) in co-digestion
443 with sludge.

444

445 To illustrate the associations, the Figure 6 depicts the mean values of the microbial
446 activity and metabolite degradation rate according to the feeding types at day 21.
447 Microorganisms and metabolites showing the same evolution in the different feeding mixtures
448 are clustered together. Similar trends were observed at the other dates (see supplemental
449 figure S4). The quality of the clustering was further assessed by comparing the proportionality
450 distances between profiles (Bodein et al., 2019; Quinn et al., 2017). The distances were lower
451 between profiles grouped within the same cluster, compared to the distances with the profiles
452 assigned to other clusters (supplemental Figure S3 and Table S3). This result confirmed a
453 strong association between the profiles of the active microorganisms and metabolites across
454 all feeding types, and their links were further investigated.

455 The microorganisms and metabolites assigned to the five clusters are described in the
456 supplemental Tables S3 and S4. Group 1 included microorganisms and metabolites with a
457 high microbial activity and high metabolite degradation rate during the digestion of sludge
458 and grass. Groups 2 to 4 included microorganisms and metabolites that were specific of either
459 sludge, grass, or fish, respectively. Finally, group 5 included the microorganisms and
460 metabolites that were highly active and highly degraded, respectively, in fish and sludge
461 bioreactors.

462 Group 1 included two genera of archaea, *Methanosarcina* and *Methanospirillum*, and
463 the metabolites diethylthiophosphate and N-(3-methylbutyl)acetamide (X153). As mentioned
464 before, diethylthiophosphate is a pesticide degradation product found in urine (Nomura et al.,
465 2014) while acetamides are produced in the fermentation of vegetal matter. One hypothesis
466 explaining the association between these archaea and metabolites could be an indirect role of
467 the archaea in the metabolites degradation through a syntrophic interaction with bacteria. This
468 is the first time such association is reported, and further investigations are required.

469 Group 2 included 14 OTUs from the orders *Cloacimonadales*, *Clostridiales*,
470 *Anaerolineales*, *Synergistales*, *Bacteroidales*, *Hydrogenedentiales* and
471 *Coprothermobacterales*, and 8 metabolites including compounds from tryptophan degradation
472 (L-tryptophanol and tryptamine, X217 and X269, respectively), 6-methylquinoline and
473 thioxoacetic acid, among others. In agreement with these metabolites, *Anaerolineales* and
474 *Synergistales* are known for their ability to degrade amino acids (Swiatczak et al., 2017).
475 Thus, their correlation with L-tryptophanol and tryptamine is consistent with the literature.
476 Surprisingly, no methanogen was identified in this group as we would have expected to find
477 with these syntrophic bacteria. One reason could be that the methanogens were not specific
478 partners of these bacteria. Indeed, most of the methanogens were found ubiquitously in
479 bioreactors fed partly with either sludge or grass (groups 2 and 3) as shown in Figure 4.

480 In group 3, 12 OTUs mostly from the orders *Clostridiales*, *Lactobacillales*,
481 *Bacteroidales* and *Spirochaetales* and the archaea *Methanofollis* were found associated with 7
482 metabolites from sugar degradation, (galactitol), lignin compounds (p-coumaric, trans-ferulic
483 acid), plant constituent (betaine) or histidine degradation (Imidazolepropionic acid). From this
484 group, it is worth noting the association between the microbial activity of the lactic acid
485 bacteria *Lactobacillales* and the degradation of lignin compounds such as trans-ferulic acid
486 (X388) and p-coumaric acid (X365). Indeed, such microorganisms are lignin degraders
487 (Fessard and Remize, 2017; Filannino et al., 2014).

488 In group 4, *Methanosarcina* and 2 OTUs from the order *Clostridiales* and metabolites
489 classified as amino acids degradation products were identified. Cadaverine (X132) and 5-
490 aminopentanoic acid (X208) are obtained from L-lysine degradation, histamine (X150) from
491 L-histidine degradation, and phenylpyruvic acid (X300) from L-phenylalanine degradation.
492 The presumed role of these microorganisms in the degradation of cadaverine and L-histidine
493 can be supported by previous studies. Roeder and Schink described a new strain close to

494 *Clostridium aminobutyricum*, able to degrade cadaverine, in co-culture with the archaea
495 *Methanospirillum* (Roeder and Schink, 2009). Some *Clostridium* were also identified to be
496 involved in the histamine degradation (Pugin et al., 2017).

497 In Group 5, heptane-1,2,3-triol and hexadecandiperoxoic acid were found to be
498 descriptive of this cluster. The origin of these metabolites is unclear and must be further
499 investigated. *Methanoculleus* and *Methanobacterium* were correlated to the genus
500 *Syntrophomonas*. Some species of this bacterium are known to growth in syntrophy with H₂-
501 consumer as methanogens (Mcinerney et al., 1981).

502 Thus, the refinement of our clusters has highlighted potentially relevant associations
503 between molecules degradation and microbial activity across different feeding substrates. This
504 is the first time that such extensive data integration analysis is performed in anaerobic
505 digestion. Previous multi-omics studies only considered single omics analysis (Beale et al.,
506 2016; Bize et al., 2015; Joyce et al., 2018).

507 Our analytical workflow suggests relationships between the degradation of metabolites
508 by different microorganisms. These relationships were consistent with the literature and future
509 work will be carried out to validate them. For instance, the degradation of the metabolites by
510 the identified microorganisms could be confirmed with either microbial cultures using these
511 specific metabolites as substrates, or by performing experiments with labelled metabolites,
512 such as stable isotope probing (Chapleur et al., 2016).

513

514 **Conclusion**

515 This study proposed a suite of statistical tools to unravel associations between
516 molecules degradation and microbial activity, whilst carefully preventing spurious
517 correlations between them. We applied component-based approaches for variable selection
518 and data integration, then further evaluated the clusters of variables using proportionality

519 distances. Our analyses show the existence of links between the anaerobic digester feeding
520 composition and microbiota activity. The associations identified between the microorganisms'
521 activity and the degradation of metabolites were biologically relevant and consistent with
522 previous literature. The statistical framework we developed in this study are promising for the
523 the screening analysis of potential metabolites degraders in different complex ecosystems
524 such as other bioprocesses, or human microbiota.

525

526 **Disclosures**

527 The authors declare no competing financial interest

528

529 **Funding**

530 This work was supported by the National Research Agency (grant number ANR-16-
531 CE05-0014) as part of the Digestomic project. Kim Anh Lê Cao, Olivier Chapleur and
532 Laëtitia Cardona scientific travels were supported in part by the France-Australia Science
533 Innovation Collaboration (FASIC) Program Early Career Fellowships from the Australian
534 Academy of Science (grant number 39417TM). Kim Anh Lê Cao was supported in part by the
535 National Health and Medical Research Council (NHMRC) Career Development fellowship
536 (grant number GNT1159458).

537

538 **Acknowledgements**

539 We thank Nadine Derlet from the Irstea PROSE analytical division for her technical
540 support. We acknowledge SUEZ Environment for providing us the access to the wastewater
541 treatment plant of Valenton.

542

543 **References**

- 544 Amha, Y.M., Anwar, M.Z., Brower, A., Jacobsen, C.S., Stadler, L.B., Webster, T.M., Smith,
545 A.L., 2018. Inhibition of anaerobic digestion processes: Applications of molecular tools.
546 *Bioresour. Technol.* 247, 999–1014. <https://doi.org/10.1016/j.biortech.2017.08.210>
- 547 Askenazi, M., Driggers, E.M., Holtzman, D.A., Norman, T.C., Iverson, S., Zimmer, D.P.,
548 Boers, M.-E., Blomquist, P.R., Martinez, E.J., Monreal, A.W., Feibelman, T.P.,
549 Mayorga, M.E., Maxon, M.E., Sykes, K., Tobin, J.V., Cordero, E., Salama, S.R.,
550 Trueheart, J., Royer, J.C., Madden, K.T., 2003. Integrating transcriptional and metabolite
551 profiles to direct the engineering of lovastatin-producing fungal strains. *Nat. Biotechnol.*
552 21, 150–156. <https://doi.org/10.1038/nbt781>
- 553 Beale, D.J., Karpe, A. V., McLeod, J.D., Gondalia, S. V., Muster, T.H., Othman, M.Z.,
554 Palombo, E.A., Joshi, D., 2016. An “omics” approach towards the characterisation of
555 laboratory scale anaerobic digesters treating municipal sewage sludge. *Water Res.*
556 <https://doi.org/10.1016/j.watres.2015.10.029>
- 557 Bize, A., Cardona, L., Desmond-Le Quéméner, E., Battimelli, A., Badalato, N., Bureau, C.,
558 Madigou, C., Chevret, D., Guillot, A., Monnet, V., Godon, J.J., Bouchez, T., 2015.
559 Shotgun metaproteomic profiling of biomimetic anaerobic digestion processes treating
560 sewage sludge. *Proteomics* 15, 3532–3543. <https://doi.org/10.1002/pmic.201500041>
- 561 Bodein, A., Chapleur, O., Droit, A., Lê Cao, K.A., 2019. A generic multivariate framework
562 for the integration of microbiome longitudinal studies with other data types. *bioRxiv* 34,
563 585802.
- 564 Bouhleb, J., Jouan-Rimbaud Bouveresse, D., Abouelkaram, S., Baéza, E., Jondreville, C.,
565 Travel, A., Ratel, J., Engel, E., Rutledge, D.N., 2018. Comparison of common
566 components analysis with principal components analysis and independent components
567 analysis: Application to SPME-GC-MS volatolomic signatures. *Talanta* 178, 854–863.

- 568 <https://doi.org/10.1016/j.talanta.2017.10.025>
- 569 Cai, M., Wilkins, D., Chen, J., Ng, S.K., Lu, H., Jia, Y., Lee, P.K.H., 2016. Metagenomic
570 reconstruction of key anaerobic digestion pathways in municipal sludge and industrial
571 wastewater biogas-producing systems. *Front. Microbiol.* 7.
572 <https://doi.org/10.3389/fmicb.2016.00778>
- 573 Callahan, B.J., Sankaran, K., Fukuyama, J.A., McMurdie, P.J., Holmes, S.P., 2016.
574 Bioconductor Workflow for Microbiome Data Analysis: from raw reads to community
575 analyses. *F1000Research* 5, 1492. <https://doi.org/10.12688/f1000research.8986.2>
- 576 Calusinska, M., Goux, X., Fossépré, M., Muller, E.E.L., Wilmes, P., Delfosse, P., 2018. A
577 year of monitoring 20 mesophilic full - scale bioreactors reveals the existence of stable
578 but different core microbiomes in bio - waste and wastewater anaerobic digestion
579 systems. *Biotechnol. Biofuels* 11. [https://doi.org/https://doi.org/10.1186/s13068-018-](https://doi.org/https://doi.org/10.1186/s13068-018-1195-8)
580 [1195-8](https://doi.org/https://doi.org/10.1186/s13068-018-1195-8)
- 581 Carballa, M., Regueiro, L., Lema, J.M., 2015. Microbial management of anaerobic digestion:
582 Exploiting the microbiome-functionality nexus. *Curr. Opin. Biotechnol.* 33, 103–111.
583 <https://doi.org/10.1016/j.copbio.2015.01.008>
- 584 Cardona, L., Levrard, C., Guenne, A., Chapleur, O., Mazéas, L., 2019. Co-digestion of
585 wastewater sludge: choosing the optimal blend. *Chem. Eng. J.* 87, 772–781.
586 <https://doi.org/10.1016/j.wasman.2019.03.016>
- 587 Chapleur, O., Mazeas, L., Godon, J.J., Bouchez, T., 2016. Asymmetrical response of
588 anaerobic digestion microbiota to temperature changes. *Appl. Microbiol. Biotechnol.*
589 100, 1445–1457. <https://doi.org/10.1007/s00253-015-7046-7>
- 590 De Francisci, D., Kougiyas, P.G., Treu, L., Campanaro, S., Angelidaki, I., 2015. Microbial
591 diversity and dynamicity of biogas reactors due to radical changes of feedstock
592 composition. *Bioresour. Technol.* <https://doi.org/10.1016/j.biortech.2014.10.126>

- 593 De Vrieze, J., Pinto, A.J., Sloan, W.T., Boon, N., Ijaz, U.Z., 2018. The active microbial
594 community more accurately reflects the anaerobic digestion process : 16S rRNA (gene)
595 sequencing as a predictive tool. *Microbiome* 1–13.
596 <https://doi.org/doi.org/10.1186/s40168-018-0449-9>
- 597 De Vrieze, J., Verstraete, W., 2016. Perspectives for microbial community composition in
598 anaerobic digestion: from abundance and activity to connectivity. *Environ. Microbiol.*
599 18, 2797–2809. <https://doi.org/10.1111/1462-2920.13437>
- 600 Escudié, F., Auer, L., Bernard, M., Mariadassou, M., Cauquil, L., Vidal, K., Maman, S.,
601 Hernandez-Raquet, G., Combes, S., Pascal, G., 2018. FROGS: Find, Rapidly, OTUs
602 with Galaxy Solution. *Bioinformatics* 34, 1287–1294.
- 603 Fahy, E., Sud, M., Cotter, D., Subramaniam, S., 2007. LIPID MAPS online tools for lipid
604 research. *Nucleic Acids Res.* 35, 606–612. <https://doi.org/10.1093/nar/gkm324>
- 605 Fessard, A., Remize, F., 2017. Why Are *Weissella* spp. Not Used as Commercial Starter
606 Cultures for Food Fermentation? *Fermentation* 3, 38.
607 <https://doi.org/10.3390/fermentation3030038>
- 608 Filannino, P., Gobbetti, M., Angelis, M. De, Cagno, R. Di, 2014. Hydroxycinnamic Acids
609 Used as External Acceptors of Electrons : an Energetic Advantage for Strictly
610 Heterofermentative Lactic Acid Bacteria 80, 7574–7582.
611 <https://doi.org/10.1128/AEM.02413-14>
- 612 Gagliano, M.C., Braguglia, C.M., Petruccioli, M., Rossetti, S., 2015. Ecology and
613 biotechnological potential of the thermophilic fermentative *Coprothermobacter* spp.
614 *FEMS Microbiol. Ecol.* 91, 1–12. <https://doi.org/10.1093/femsec/fiv018>
- 615 González, I., Lê Cao, K.-A., Davis, M.J., Déjean, S., 2012. Visualising associations between
616 paired ‘omics’ data sets. *BioData Min.* 5, 19. <https://doi.org/10.1186/1756-0381-5-19>
- 617 Han, J., Meng, J., Chen, S., Li, C., 2019. Integrative analysis of the gut microbiota and

- 618 metabolome in rats treated with rice straw biochar by 16S rRNA gene sequencing and
619 LC/MS-based metabolomics. *Sci. Rep.* 9, 1–9. [https://doi.org/10.1038/s41598-019-](https://doi.org/10.1038/s41598-019-54467-6)
620 [54467-6](https://doi.org/10.1038/s41598-019-54467-6)
- 621 Hassa, J., Maus, I., Off, S., Pühler, A., Scherer, P., Klocke, M., Schlüter, A., 2018.
622 Metagenome, metatranscriptome, and metaproteome approaches unraveled compositions
623 and functional relationships of microbial communities residing in biogas plants. *Appl.*
624 *Microbiol. Biotechnol.* 102, 5045–5063. <https://doi.org/10.1007/s00253-018-8976-7>
- 625 Hoefgen, R., Nikiforova, V.J., 2008. Metabolomics integrated with transcriptomics: Assessing
626 systems response to sulfur-deficiency stress. *Physiol. Plant.* 132, 190–198.
627 <https://doi.org/10.1111/j.1399-3054.2007.01012.x>
- 628 Horai, H., Arita, M., Kanaya, S., Nihei, Y., Ikeda, T., Suwa, K., Ojima, Y., Tanaka, Kenichi,
629 Tanaka, S., Aoshima, K., Oda, Y., Kakazu, Y., Kusano, M., Tohge, T., Matsuda, F.,
630 Sawada, Y., Hirai, M.Y., Nakanishi, H., Ikeda, K., Akimoto, N., Maoka, T., Takahashi,
631 H., Ara, T., Sakurai, N., Suzuki, H., Shibata, D., Neumann, S., Iida, T., Tanaka, Ken,
632 Funatsu, K., Matsuura, F., Soga, T., Taguchi, R., Saito, K., Nishioka, T., 2010.
633 MassBank: A public repository for sharing mass spectral data for life sciences. *J. Mass*
634 *Spectrom.* 45, 703–714. <https://doi.org/10.1002/jms.1777>
- 635 Ito, T., Yoshiguchi, K., Ariesyady, H.D., Okabe, S., 2011. Identification of a novel acetate-
636 utilizing bacterium belonging to Synergistes group 4 in anaerobic digester sludge. *ISME*
637 *J.* 5, 1844–1856. <https://doi.org/10.1038/ismej.2011.59>
- 638 Jiang, M., Wang, C., Zhang, Y., Feng, Y., Wang, Y., Zhu, Y., 2014. Sparse Partial-least-
639 squares Discriminant Analysis for Different Geographical Origins of *Salvia miltiorrhiza*
640 by 1 H-NMR-based Metabolomics. *Phytochem. Anal.* 25, 50–58.
641 <https://doi.org/10.1002/pca.2461>
- 642 Joyce, A., Ijaz, U.Z., Nzeteu, C., Vaughan, A., Shirran, S.L., Botting, C.H., Quince, C.,

- 643 O’Flaherty, V., Abram, F., 2018. Linking microbial community structure and function
644 during the acidified anaerobic digestion of grass. *Front. Microbiol.* 9, 1–13.
645 <https://doi.org/10.3389/fmicb.2018.00540>
- 646 Lê Cao, K.-A., Boitard, S., Besse, P., 2011. Sparse PLS discriminant analysis: biologically
647 relevant feature selection and graphical displays for multiclass problems. *BMC*
648 *Bioinformatics* 12, 253. <https://doi.org/10.1186/1471-2105-12-253>
- 649 Lê Cao, K.-A., Martin, P.G., Robert-Granié, C., Besse, P., 2009. Sparse canonical methods
650 for biological data integration: application to a cross-platform study. *BMC*
651 *Bioinformatics* 10, 34. <https://doi.org/10.1186/1471-2105-10-34>
- 652 Lee, J., Kim, E., Han, G., Tongco, J.V., Shin, S.G., Hwang, S., 2018. Microbial communities
653 underpinning mesophilic anaerobic digesters treating food wastewater or sewage sludge:
654 A full-scale study. *Bioresour. Technol.* 259, 388–397.
655 <https://doi.org/10.1016/j.biortech.2018.03.052>
- 656 Li, N., He, J., Yan, H., Chen, S., Dai, X., 2017. Pathways in bacterial and archaeal
657 communities dictated by ammonium stress in a high solid anaerobic digester with
658 dewatered sludge. *Bioresour. Technol.* 241, 95–102.
659 <https://doi.org/10.1016/j.biortech.2017.05.094>
- 660 Longnecker, K., Futrelle, J., Coburn, E., Kido, M.C., Kujawinski, E.B., 2015. Environmental
661 metabolomics : Databases and tools for data analysis. *Mar. Chem.* 177, 366–373.
662 <https://doi.org/10.1016/j.marchem.2015.06.012>
- 663 Lü, F., Bize, A., Guillot, A., Monnet, V., Madigou, C., Chapleur, O., Mazéas, L., He, P.,
664 Bouchez, T., 2014. Metaproteomics of cellulose methanisation under thermophilic
665 conditions reveals a surprisingly high proteolytic activity. *ISME J.* 8, 88–102.
666 <https://doi.org/10.1038/ismej.2013.120>
- 667 Madigou, C., Lê Cao, K.-A., Bureau, C., Mazéas, L., Déjean, S., Chapleur, O., 2019.

- 668 Ecological consequences of abrupt temperature changes in anaerobic digesters. *Chem.*
669 *Eng. J.* 361, 266–277. <https://doi.org/10.1016/J.CEJ.2018.12.003>
- 670 McHardy, I.H., Goudarzi, M., Tong, M., Ruegger, P.M., Schwager, E., Weger, J.R., Graeber,
671 T.G., Sonnenburg, J.L., Horvath, S., Huttenhower, C., McGovern, D.P., Fornace, A.J.,
672 Borneman, J., Braun, J., 2013. Integrative analysis of the microbiome and metabolome of
673 the human intestinal mucosal surface reveals exquisite inter-relationships. *Microbiome* 1,
674 17. <https://doi.org/10.1186/2049-2618-1-17>
- 675 Mcinerney, M.J., Bryant, M.P., Hespell, R.B., Costerton, J.W., 1981. *Syntrophomonas wolfei*
676 *gen. nov. sp. nov.*, an Anaerobic, Syntrophic, Fatty Acid-Oxidizing Bacterium 41, 1029–
677 1039.
- 678 Nobu, M.K., Narihiro, T., Rinke, C., Kamagata, Y., Tringe, S.G., Woyke, T., Liu, W., 2015.
679 Microbial dark matter ecogenomics reveals complex synergistic networks in a
680 methanogenic bioreactor. *ISME J.* 9, 1710–1722.
681 <https://doi.org/https://doi.org/10.1038/ismej.2014.256>
- 682 Noll, M., Klose, M., Conrad, R., 2010. Effect of temperature change on the composition of
683 the bacterial and archaeal community potentially involved in the turnover of acetate and
684 propionate in methanogenic rice field soil. *FEMS Microbiol. Ecol.* 73, 215–25.
685 <https://doi.org/10.1111/j.1574-6941.2010.00883.x>
- 686 Nomura, H., Ueyama, J., Sugiura, Y., Takaiishi, A., Hayashi, Y., Kondo, T., Inuzuka, K.,
687 Kamijima, M., Ogi, H., Osaka, A., Inoue, M., Wakusawa, S., Saito, I., 2014. A revised
688 method for determination of dialkylphosphate levels in human urine by solid-phase
689 extraction and liquid chromatography with tandem mass spectrometry: application to
690 human urine samples from Japanese children. *Environ. Health Prev. Med.* 19, 405–413.
691 <https://doi.org/10.1007/s12199-014-0407-5>
- 692 Poirier, S., Bize, A., Bureau, C., Bouchez, T., Chapleur, O., 2016. Community shifts within

- 693 anaerobic digestion microbiota facing phenol inhibition: Towards early warning
694 microbial indicators? *Water Res.* 100, 296–305.
695 <https://doi.org/10.1016/j.watres.2016.05.041>
- 696 Pugin, B., O’Mahony, L., Westermann, P., Hellings, P., Wawrzyniak, M., Heider, A., Akdis,
697 C.A., Barcik, W., 2017. A wide diversity of bacteria from the human gut produces and
698 degrades biogenic amines. *Microb. Ecol. Health Dis.* 28, 1353881.
699 <https://doi.org/10.1080/16512235.2017.1353881>
- 700 Quinn, T.P., Richardson, M.F., Lovell, D., Crowley, T.M., 2017. Propr: An R-package for
701 Identifying Proportionally Abundant Features Using Compositional Data Analysis. *Sci.*
702 *Rep.* 7, 1–9. <https://doi.org/10.1038/s41598-017-16520-0>
- 703 Roeder, J., Schink, B., 2009. Syntrophic degradation of cadaverine by a defined methanogenic
704 coculture. *Appl. Environ. Microbiol.* 75, 4821–4828.
705 <https://doi.org/10.1128/AEM.00342-09>
- 706 Rohart, F., Gautier, B., Singh, A., Cao, K.-A. Le, 2017. mixOmics: an R package for ’omics
707 feature selection and multiple data integration. *bioRxiv* 108597.
708 <https://doi.org/10.1101/108597>
- 709 Sekiguchi, Y., Takahashi, H., Kamagata, Y., Ohashi, A., Harada, H., 2001. In Situ Detection,
710 Isolation, and Physiological Properties of a Thin Filamentous Microorganism Abundant
711 in Methanogenic Granular Sludges: a Novel Isolate Affiliated with a Clone Cluster, the
712 Green Non-Sulfur Bacteria, Subdivision I. *Appl. Environ. Microbiol.* 67, 5740–5749.
713 <https://doi.org/10.1128/AEM.67.12.5740>
- 714 Shen, H., Huang, J.Z., 2008. Sparse principal component analysis via regularized low rank
715 matrix approximation. *J. Multivar. Anal.* 99, 1015–1034.
716 <https://doi.org/10.1016/j.jmva.2007.06.007>
- 717 Singh, A., Benoît, G., Shannon, C.P., Vacher, M., Rohart, F., Tebbutt, S.J., Lê Cao, K.-A.,

- 718 2019. DIABLO: an integrative, multi-omics, multivariate method for multi-group
719 classification. *Bioinformatics* 1–50.
720 <https://doi.org/https://doi.org/10.1093/bioinformatics/bty1054>
- 721 Smith, C.A., Want, E.J., Maille, G.O., Abagyan, R., Siuzdak, G., 2006. XCMS : Processing
722 Mass Spectrometry Data for Metabolite Profiling Using Nonlinear Peak Alignment ,
723 Matching , and Identification. *Anal. chemistry* 78, 779–787.
- 724 Sousa, D.Z., Salvador, A.F., Ramos, J., Guedes, A.P., Barbosa, S., Stams, A.J.M., Alves,
725 M.M., Pereira, M.A., 2013. Activity and viability of methanogens in anaerobic digestion
726 of unsaturated and saturated long-chain fatty acids. *Appl. Environ. Microbiol.* 79, 4239–
727 4245. <https://doi.org/10.1128/AEM.00035-13>
- 728 Straube, J., Huang, B.E., Lê Cao, K.-A., 2017. DynOmics to identify delays and co-
729 expression patterns across time course experiments. *Sci. Rep.* 7, 1–11.
730 <https://doi.org/10.1038/srep40131>
- 731 Swiatczak, P., Cydzik-Kwiatkowska, A., Rusanowska, P., 2017. Microbiota of anaerobic
732 digesters in a full-scale wastewater treatment plant. *Arch. Environ. Prot.* 43, 53–60.
733 <https://doi.org/10.1515/aep-2017-0033>
- 734 Vanwonterghem, I., Jensen, P.D., Ho, D.P., Batstone, D.J., Tyson, G.W., 2014. Linking
735 microbial community structure, interactions and function in anaerobic digesters using
736 new molecular techniques. *Curr. Opin. Biotechnol.* 27, 55–64.
737 <https://doi.org/10.1016/j.copbio.2013.11.004>
- 738 Villas-Bôas, S.G., Noel, S., Lane, G.A., Attwood, G., Cookson, A., 2006. Extracellular
739 metabolomics: A metabolic footprinting approach to assess fiber degradation in complex
740 media. *Anal. Biochem.* 349, 297–305. <https://doi.org/10.1016/j.ab.2005.11.019>
- 741 Wang, M., Zhang, X., Zhou, J., Yuan, Y., Dai, Y., Li, D., Li, Z., Liu, X., Yan, Z., 2017. The
742 dynamic changes and interactional networks of prokaryotic community between co-

743 digestion and mono-digestions of corn stalk and pig manure. *Bioresour. Technol.* 225,
744 23–33. <https://doi.org/10.1016/j.biortech.2016.11.008>

745 Wishart, D.S., Feunang, Y.D., Marcu, A., Guo, A.C., Liang, K., Vázquez-Fresno, R., Sajed,
746 T., Johnson, D., Li, C., Karu, N., Sayeeda, Z., Lo, E., Assempour, N., Berjanskii, M.,
747 Singhal, S., Arndt, D., Liang, Y., Badran, H., Grant, J., Serra-Cayuela, A., Liu, Y.,
748 Mandal, R., Neveu, V., Pon, A., Knox, C., Wilson, M., Manach, C., Scalbert, A., 2018.
749 HMDB 4.0: The human metabolome database for 2018. *Nucleic Acids Res.* 46, D608–
750 D617. <https://doi.org/10.1093/nar/gkx1089>

751 Zamanzadeh, M., Hagen, L.H., Svensson, K., Linjordet, R., Horn, S.J., 2017. Biogas
752 production from food waste via co-digestion and digestion- effects on performance and
753 microbial ecology. *Sci. Rep.* 7, 1–12. <https://doi.org/10.1038/s41598-017-15784-w>

754